Characterization of Nanocomposite Laminates Fabricated from Aqueous Dispersion of Nanoclay

Levent Aktas, M. Cengiz Altan
School of Aerospace and Mechanical Engineering, University of Oklahoma, Norman, Oklahoma

Preparation of E-glass/waterborne epoxy prepregs containing natural nanoclay and properties of their composites are presented. Prepregs were prepared by wetting randomly oriented, chopped glass fiber preforms with aqueous dispersion of EpiRez 3522-W-60 resin, dicyandiamide, 2-methylimidazole and natural nanoclay (Cloisite® Na^+). The nanoclay content of the aqueous dispersion was adjusted to yield final nanoclay contents of 0, 1, 2, and 4 wt%, whereas the glass fiber content is kept constant at 47 wt%. These prepregs were then used to fabricate disk-shaped composite samples by APA2000 rheometer. Composite samples were tested for interlaminar shear strength, flexural stiffness, and glass transition temperature. The flexural stiffness was observed to increase by more than 26% over the range of nanoclay loading, despite a 13% decrease in interlaminar shear strength. Similarly, glass transition temperature increased from 89°C to above 94°C for the samples comprising 4 wt% nanoclay. X-ray diffraction analyses indicated 48% increase in the gallery spacing suggesting strong intercalation of the nanoclay platelets by the epoxy matrix. Microstructural observations of the fracture surfaces and polished surfaces show significant differences in the matrix topology and fiber to matrix adhesion. The composites with higher nanoclay content depict uniform and submicron surface features implying homogenous dispersion of nanoclay. POLYM. COMPOS., 31:620–629, 2010. © 2009 Society of Plastics Engineers

INTRODUCTION

During the last two decades, particulates with nanometer scale features—so-called nanoparticulates—are utilized to improve the physical and mechanical properties of polymers and composites [1]. Among the nanoparticulates, carbon nanotubes and nanoclay have been widely studied. In particular, nanoclay is preferred in commercial applications over carbon nanotubes owing to its low-cost and abundance [2–4].

Correspondence to: M. Cengiz Altan; e-mail: altan@ou.edu
DOI 10.1002/pc.20837
Published online in Wiley InterScience (www.interscience.wiley.com).

Since its first implementation by the research group at Toyota Research Labs [5–7], several studies reported improvements in various thermo-mechanical properties of thermoplastics containing nanoclay. Among these properties, the most drastic changes were observed in mechanical [7–9], thermal [10, 11], and barrier properties [12, 13]. For instance, Kojima et al. [7] reported an increase in flexural strength and flexural stiffness of nylon 6 from 89.3 MPa to 143 MPa and from 1.94 GPa to 4.34 GPa with 4.7 wt% nanoclay loading. Similarly, Maiti et al. [14] investigated the effect of nanoclay on the high temperature dynamic mechanical properties of polypropylene. Maleic anhydride grafted polypropylene (PP-MA) was blended with cation-exchanged nanoclay at loadings ranging from 2 to 7.5 wt% and melt extruded. Over the range of nanoclay loading, the storage modulus of polypropylene is observed to increase by 156 and 164% at 70 and 130°C, respectively.

In addition to neat polymers, nanoclay is also used in fabrication of fiber reinforced composites. A number of researchers used nanoclay in the glass/epoxy [15–17] and carbon/epoxy [18–20] composites. For example, Haque et al. [15] added Nanomer® I.28E nanoclay into glass/epoxy composites. The authors blended 1, 2, 5, and 10 wt% of nanoclay into epoxy resin, mixed with curing agent and fabricated nanocomposite samples reinforced with woven glass fiber preforms by vacuum assisted resin infusion method (VARIM). Thermogravimetric analysis indicated that the addition of 1 wt% nanoclay increased the onset of decomposition temperature by 10.6%. However, may be due to agglomeration, at higher clay contents the thermal properties were observed to degrade.

The improvements in mechanical properties were most frequently observed for the rubbery epoxy matrices. For instance, Lan and Pinnavaia [21] reported 18- and 12-fold improvements in the tensile strength and stiffness of an epoxy matrix with the addition of 23.2 wt% nanoclay. However, the authors also mention that the choice of curing agent resulted in a rubbery epoxy matrix before the clay was added. According to the authors, the property improvements observed in glassy epoxies were marginal. Similar to Lan and Pinnavaia [21], Boukerrou et al. [22] investigated the utility of nanoclay with DGEBA epoxy

resin. Even though TEM images indicated nanoclay aggregates with sizes in the order of 2–5 μm, the tensile strength and stiffness of the epoxy resin were observed to increase by 39 and 36%, respectively. The authors [22] also report that the epoxy system was rubbery at ambient temperature and the glass transition temperature was -30°C. Lan and Pinnavaia [21] and others suggested reinforcement mechanisms that result in improved properties in rubbery polymers. According to Lan and Pinnavaia, the reinforcement effect of nanoclay in rubbery polymers is due to the large deformations encountered before failure. During those deformations the clay platelets are most likely forced to align in the direction of the force and act as reinforcing elements.

Among the studies dealing with glassy epoxy matrices, Abot et al. [23] studied adding two commercially available nanoclays, Cloisite® 30B and Nanomer® I.28E, in an epoxy resin. The authors reported 28% reduction in tensile strength despite a 31% increase in tensile stiffness. In addition, up to 28% reduction in glass transition temperature was reported. Although x-ray diffraction studies indicated complete exfoliation for Cloisite® 30B and intercalation for Nanomer® I.28E, the scanning electron microscope images indicated nanoclay tactoids as large as 10 μm. On the other hand, Wang et al. [24] implemented surface treated nanoclay with DGEBA epoxy resin at loadings ranging from 1 to 5 wt%. It is observed that the tensile stiffness monotonically increased from 2 GPa for the neat epoxy to 2.7 GPa for the nanocomposite containing 5 wt% nanoclay. In the same loading range, the tensile strength decreased by as much as 30%.

Aside from the improvements in the mechanical properties of weak, rubbery polymers, the improvement in the properties of epoxy resins and fiber reinforced composites using nanoclay are less frequently reported in the literature compared to thermoplastics. The most likely reason for not achieving substantial improvements in epoxy resins is insufficient dispersion of the nanoclay clusters within the matrix. To overcome the problem of dispersion, the natural nanoclay is often subjected to cation exchange reaction to alter its surface properties from hydrophilic to organophilic. Even though there is a wide range of organically modified nanoclays available and various mixing techniques exist, the formation of nanoclay clusters has been widely reported. Second, during the processing of thermoplastic polymers, the nanoclay clusters are subjected to higher shear forces, which helps to break down the nanoclay clusters [8]. Such high shear forces are often not present during processing of thermosetting polymers with lower viscosity.

An alternative approach for dispersing nanoclay in epoxy matrices may be the utilization of waterborne epoxies. As has been studied extensively by earth scientists, natural clay is strongly hydrophilic [25]. Furthermore, sodium montmorillonite—the particular clay type often used in nanocomposite applications—is expected to disperse close to individual platelet level [25] when mixed with water. Therefore utilization of natural nanoclay with waterborne epoxy resins may serve as a viable solution to achieve complete dispersion.

There are a number of advantages of waterborne epoxies. In a waterborne system, epoxy particles, either in solid or liquid form, are emulsified in water, thus eliminating the need for solvents. Because of its solvent-free formulation, waterborne epoxy resins are environmentally safe. Moreover, the viscosity of the waterborne systems can be controlled by the amount of water in the system, as desired [26]. Ability to control the viscosity is especially important in systems containing nanoclay, since it is known that addition of nanoclay result in abrupt increases the viscosity [27].

Using natural clay has a number of advantages over the organically modified clay. First, the natural clay is cost-effective compared with organically modified clays because the cation-exchange step is not carried out during its production. Second, it has been shown by Lan et al. [28] that epoxies may undergo self-polymerization when heated with acidic onium ion exchanged nanoclay to form polyether. This may result in a stoichiometric imbalance causing unreacted curing agent to remain in the system and thus adversely affect the properties. Park and Jana [29] later indicated that this catalytic effect of the organic modification on the clay surfaces results in plasticization of the epoxy networks and cause significant reductions in the glass transition temperature and storage modulus. More recently, our research group observed inhomogeneous sections around the nanoclay clusters in TEM images of epoxy/organically modified clay nanocomposites [30]. These areas were possibly caused by the excess curing agent left as a result of the stoichiometric imbalance created by the organically modified clay used.

In this study we present a novel method to prepare prepregs from aqueous dispersion of nanoclay, and use this method to investigate the utility of natural nanoclay with E-glass/waterborne epoxy composites. E-glass/waterborne epoxy prepregs containing 0, 1, 2, and 4% nanoclay are prepared and cured by an APA2000 rheometer. Mechanical properties of these laminates are determined by three-point bending tests whereas the quality of dispersion of nanoclay is characterized by x-ray diffraction and scanning electron microscopy.

MATERIALS AND METHODS

Batch Preparation and Prepreg Fabrication

The waterborne epoxy resin used in this study is EpiRez 3522-W-60 from Hexion Chemicals. This particular waterborne epoxy resin contains solid DGEBA particles with an average dimension in the order of 1 μm that are emulsified in water. As recommended by the supplier, Dicyandiamide (Dicy) and 2-Methylimidazole (2 MI) from Aldrich Chemicals were chosen as the curing agents. The curing agent

was prepared by dissolving 1.2 parts of Dicy and 0.15 parts of 2 MI in 21 parts of distilled water at 70°C. The curing agent solution was vigorously agitated and sonicated for 5 min and added into 100 parts of EpiRez 3522-W-60 epoxy resin. This final compound is mixed via a mechanical mixer for 30 min before fabrication of the prepregs. Desired amounts of natural nanoclay (Cloisite® Na^+) is added into the curing agent to yield final nanoclay contents of 0, 1, 2, and 4% by weight within the epoxy matrix.

Cloisite® Na^+ is a natural, untreated montmorillonite type of clay, supplied by Southern Clay Products Inc. (Gonzales, TX). The specific gravity and mean particle size of Cloisite® Na^+ is reported as 2.86 and 6 μm, respectively, by the supplier. According to the x-ray diffraction results provided by the supplier, the gallery spacing of Cloisite® Na^+ is 11.7Å.

Randomly oriented, chopped strand E-glass fiber preforms with a planar density of 0.2280 kg/m^2 (Fiberglast, part# 248) were used for prepreg fabrication. Sheets of $6'' \times 10''$ preforms were cut from the fiber roll as shown in Fig. 1A. These sheets were then wetted with the waterborne epoxy/curing agent/nanoclay mixture. A stainless steel roller was used to squeeze out the excess resin. Figure 1B shows an E-glass preform after impregnated by waterborne epoxy/cure agent/nanoclay mixture. It can be seen in Fig. 1B that the wetted preform has a porous and flexible structure. At this stage, the wet prepreg can be draped onto a nonplanar surface before the removal of water. Before impregnation, viscosity of the waterborne epoxy/cure agent/nanoclay mixture can be tailored for the preform type, planar density, and the waive pattern such that the preform can be properly impregnated without any dry spots and trapped microvoids. Excessive clustering of nanomaterials and nonhomogeneous wetting can be also avoided by adding water as needed to reduce the viscosity.

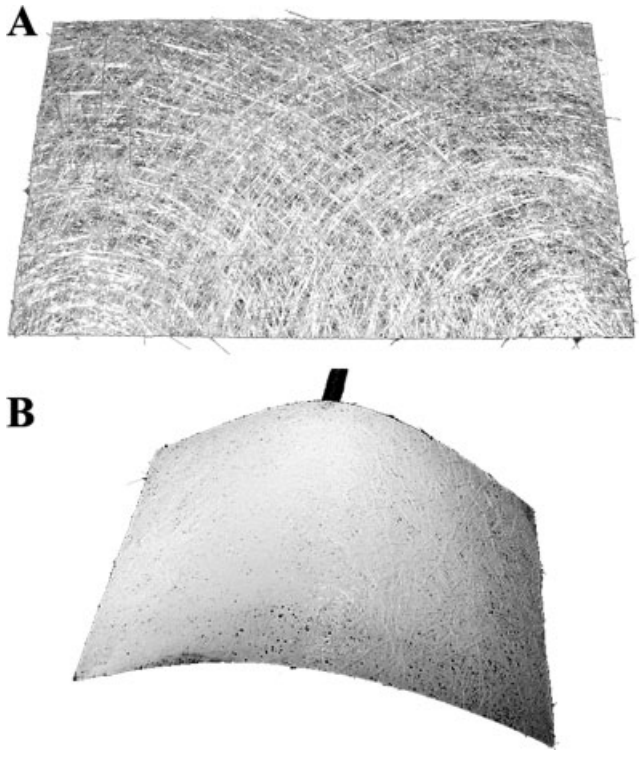

FIG. 1. Steps of prepreg fabrication. (A) Dry glass preform as received and cut to the size; (B) Drapeable glass preform wetted with epoxy/cure agent/nanoclay mixture.

Following the completion of the wetting procedure, the prepregs were placed in an oven at 120°C for 20 min to remove the water from the system. After water is removed, the glass preform becomes nontacky and much more rigid compared to its initial state. The final nontacky, rigid prepregs are kept in a freezer until the fabrication of sample laminates.

It is important to emphasize that the method presented here can be used to introduce a desired amount of nanomaterial onto a conventional prepreg. In fact, more than one type of nanomaterial can be added at varying percentages, as long as each material is dispersible in water. One can also prepare prepregs having different amounts and types of nanomaterials, which would be used later to fabricate functionally graded or functionally tailored composite laminates. Another possibility is to use these aqueous dispersions in vacuum assisted impregnation of conventional glass or graphite fabrics or mats. After the preform is impregnated, open mold curing methods can be used to fabricate geometrically complex, nanocomposite products.

The SEM images of the composite prepreg before and after cure were captured at 50× as shown in Fig. 2. The prepreg image before cure shows multiple layers of collimated glass fibers and epoxy sheets located either between fibers or as distinct thin layers. Irregular fracture surfaces or thin surface cracks on epoxy matrix are clearly visible indicating the brittleness of material at this state. Before cure image also indicates a rather uniform distribution of epoxy resin throughout the fiber bundles. The SEM image taken after the cure depicts that epoxy matrix has completely wetted glass fibers and formed a thin coating layer. Several resin beads are also visible around fibers clearly indicating formation of low contact angle drops wrapping around one or more fibers. The surface morphology observed after cure demonstrates favorable wetting of the glass fibers during cure, thus yielding a robust fiber matrix interface. Strong adhesion between the resin and the fiber dictates the effectiveness of load transfer throughout the composite, and therefore positively influences the final mechanical properties.

Sample Fabrication

Sample fabrication was performed by the dynamic mechanical analyzer, APA2000 from Alpha Technologies Inc. The unique feature of APA2000 is its ability to measure temporal evolution of viscoelastic properties, while a 3 mm-thick, disk-shaped (D = 44.5 mm) composite laminate is cured. The fabricated samples are large enough to allow further characterization such as flexural and interlaminar properties via three-point bending tests.

 DOI 10.1002/pc

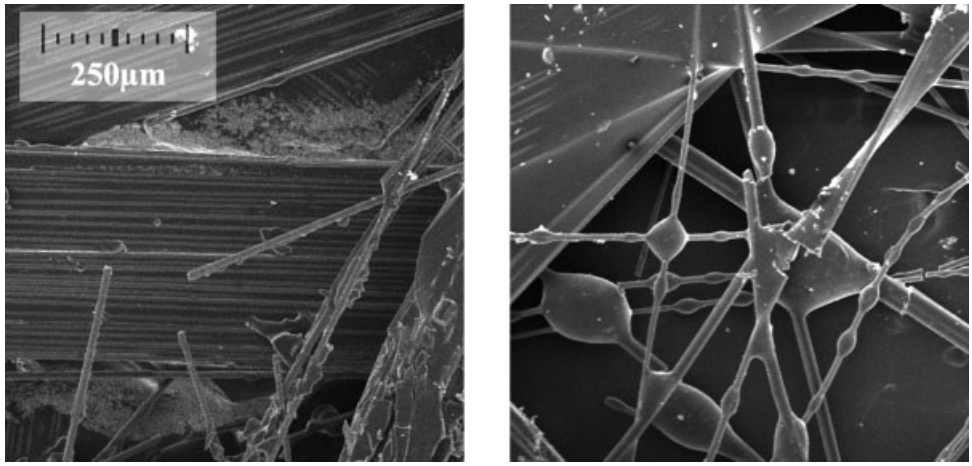

FIG. 2. SEM image taken at ×50 magnification showing surface morphology of the prepreg before cure (Left); SEM image after cure illustrating the wetting of glass fibers (Right).

To prepare cured laminate samples, 44.5 mm diameter circles were punched out of the fabricated prepregs and weighed to determine their glass fiber content. A total of 14 layers were chosen and stacked together such that all of the fabricated laminates had identical weight and glass fiber contents. These samples were enclosed by a viton o-ring and placed between nylon films before loading into the APA2000. The glass fiber content of all samples was determined to be 47 wt%. The number of layers was chosen as 14 after several trials to prevent slippage problems and avoid excess resin leaking out of the o-ring. The evolution of viscoelastic response of the laminate was measured throughout the curing process at an oscillation frequency of 1 Hz and an angular deformation of 0.05 degrees.

During curing, temperature was increased from ambient up to 176.7°C (350°F) at a rate of 5°C/min and then kept at 176.7°C for 60 min to complete curing. Upon completion of curing, temperature is reduced to 50°C at a rate of 10°C/min. To determine the glass transition temperature of the cured samples, the temperature was raised once again at a rate of 1°C/min up to 140°C and then lowered to room temperature before removing the sample. A cured sample fabricated by APA2000 is depicted in Fig. 3. Five disk-shaped samples are fabricated for each nanoclay content studied.

Upon completion of curing, two 10 mm × 28 mm rectangular samples, outlined in Fig. 3, were cut out by a precision saw with a diamond blade. A total of 10 samples were obtained for each nanoclay content with an average thickness of 3 mm. Out of those 10 samples, five of them were tested under three point bending to determine their interlaminar shear strength and the remaining five were reserved for future studies.

Rheological Analysis

The viscoelastic properties of the samples during curing were recorded by APA2000 rheometer. Storage modulus is recorded as a function of time and temperature to determine whether the fully cured state was reached for the temperature cycle used. In addition, the rheological data was used to understand the effects of nanoclay on the cure behavior of glass/waterborne epoxy composites.

Glass transition temperatures of the cured samples were determined by an additional temperature cycle mentioned earlier. The temperature where the loss tangent displayed a peak was identified as the glass transition temperature of the sample according to ASTM E1640-99 standard. The glass transition temperature was measured for all of the fabricated samples.

X-Ray Diffraction

The gallery spacing of Cloisite® Na^+ is determined by wide angle x-ray diffraction by examining under CuKα radiation. Samples for wide angle x-ray diffraction are

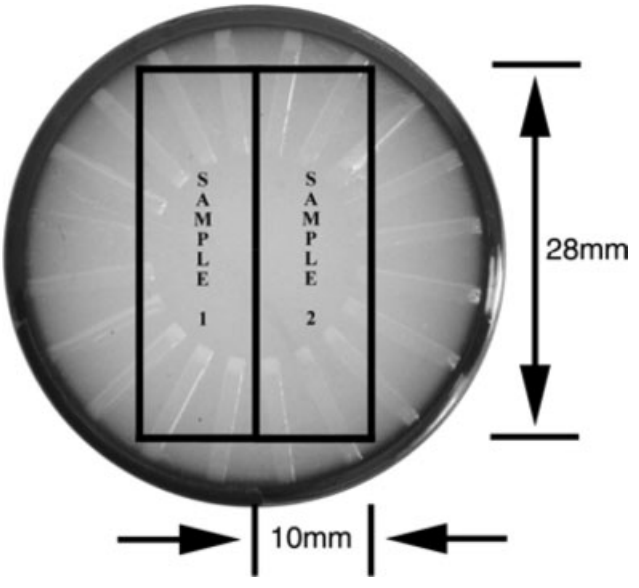

FIG. 3. Disk-shaped sample cured in APA2000.

prepared by placing a small amount of clay between two layers of scotch tape. In addition, composite samples with a thickness of 100 μm are cut from the disks for small angle x-ray diffraction to determine the change in gallery spacing of clay after fabrication of the composite parts.

Mechanical Testing

From each group of samples with different nanoclay contents, five samples were tested under three-point bending to determine their interlaminar shear strength and flexural stiffness as per ASTM D2344/D2344M-00 standard. Testing was performed by a 5-kip Com-Ten testing machine at a constant displacement rate of 2 mm/min using a 25.4 mm sample span.

Microstructural Characterization

Scanning electron microscopy is utilized to analyze the microstructure of the samples. Through-the-thickness surfaces of the samples are polished using a series of aluminum oxide lapping films down to 1 μm grit size. The samples were then coated with gold-palladium to render the surface conductive and prevent charging. Scanning electron micrographs were gathered by JEOL-880 high resolution microscope in secondary electron imaging mode at magnifications ranging from 50× to 50k×. In addition to the polished surfaces, the fracture surfaces of the mechanically tested samples are also studied under SEM to identify any change in adhesion between epoxy matrix and glass fibers because of nanoclay.

RESULTS AND DISCUSSION

Cure Kinetics

The development of the storage moduli is given in Fig. 4 along with the temperature cycle used for curing the samples. The time storage modulus starts increasing significantly is used to determine the gel time of composites. For the cure cycle used, the gel time is measured as 25 min regardless of the nanoclay content. Although the gel times of the samples are identical, the maximum storage modulus that the samples reach during curing is significantly influenced by the amount of nanoclay in the system. With increasing nanoclay content, the storage modulus increased monotonically from 325 MPa to more than 1 GPa at 4% nanoclay loading. Since the composites are dominantly elastic rather than viscous, the storage moduli measured at the end of cure can be correlated with the stiffness of the system at that temperature. Clearly, the stiffness of the system at the cure temperature of 176.7°C (350°F) improved by more than threefold because of the addition of nanoclay.

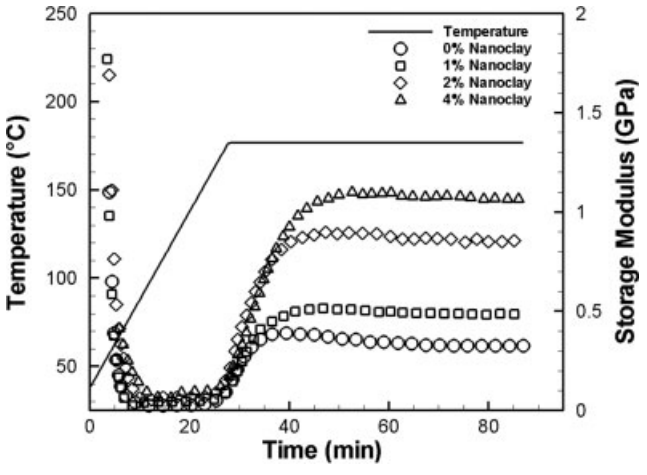

FIG. 4. Development of storage moduli during curing.

Among various alternatives, degree of cure of thermosetting polymers and composites can be described by the development of storage modulus during curing [31–33]. This is realized by normalizing the storage modulus with its plateau value at the completion of curing:

$$\propto (t) = \frac{G'(t) - G'_{\min}}{G'_{\infty} - G'_{\min}}. \quad (1)$$

In the aforementioned equation, $\propto (t)$ is the degree of cure, $G'_{\min}$ is the minimum storage modulus during cure and $G'_{\propto}$ is the plateau value of storage modulus upon completion of curing. Although the gel times of the samples with different nanoclay contents are identical, because of the difference in the plateau value of the storage moduli, the curing rates are different. For instance, samples with 0, 1, 2, and 4 wt% nanoclay reached 80% degree of cure in 32, 35, 36, and 39 min, respectively. Therefore, it can be concluded that natural nanoclay has a slight hindering effect on the cure kinetics of waterborne epoxy resins.

The effect of nanoclay on the cure kinetics of epoxy resins were not studied as widely as its effect on other physical properties. Among studies of cure behavior, Kortaberria et al. [34] investigated the cure kinetics of DGEBA epoxy resin containing Nanofil 919 (organically modified nanoclay by Süd Chemie España) by dielectric spectroscopy. The authors observed up to 35% reduction in gel time at 5% nanoclay content, indicating significantly faster curing. Similar increases in the rate of cure were also observed by Uhl et al. [35] with Nanomer I.31PS, Seo and Kim [36] with Cloisite® 30B and by Román et al. [37] with Nanomer I.30E. However, it should be noted that all these studies are conducted with organically modified nanoclay. Lan et al. [28] and Park and Jana [29] showed that the octadecylamine used in organic modifications of nanoclay may cause homopolymerization of the epoxy molecules, thus resulting in an increase in the rate of cure. In our case, because of the choice of natural nanoclay, organic modifiers are not present. Therefore, effects such as homopolymerization that may increase the curing rate are not expected. On the other hand, Kornmann et al. [38] and Ngo et al. [39] stressed the importance of molecular mobility of curing agent and

 DOI 10.1002/pc

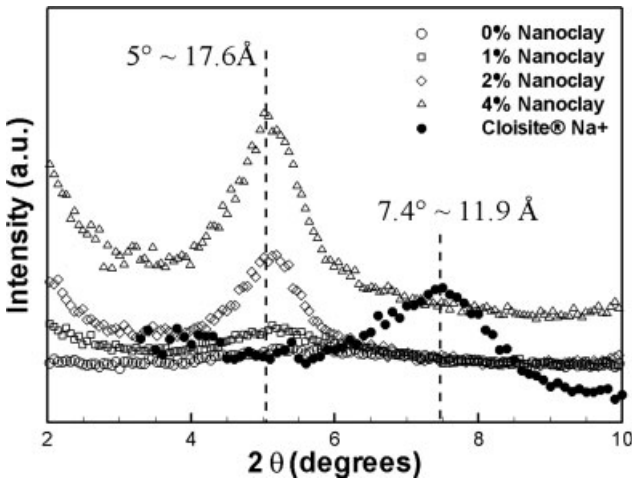

FIG. 5. X-Ray diffraction spectra of Cloisite® Na+ and composite samples with and without nanoclay.

epoxy molecules on the kinetics of cure and nanocomposite formation. This steric effect of nanoclay is most likely responsible for the reduced rate of cure observed in the current study.

X-Ray Diffraction

X-ray diffraction is preferred by the majority of researchers to describe the intercalation and exfoliation in a quantitative manner. In this method, a well characterized X-ray (most of the time CuKα) is forwarded onto the surface of interest. Based on the angle of diffraction of the X-ray emitted from the surface, the basal spacing between the nanoclay platelets is calculated through Bragg's Law [40]. Although it has been criticized for the possibility of arriving at misleading conclusions on the state of exfoliation [41], x-ray diffraction is a widely accepted method of measuring the changes in gallery spacing over a relatively large sample area.

In this study, the gallery spacing of the natural nanoclay is measured and compared with the gallery spacing of nanoclay in the composite. The results of the x-ray diffraction study are shown in Fig. 5. The diffraction peak for Cloisite® Na^+ is observed at 7.4°, which corresponds to 11.9 Å for the CuKα radiation. This value is very close to the gallery spacing of 11.7 Å reported by the material supplier, Southern Clay Products Inc [42]. The sample without nanoclay, as expected, did not display diffraction peak in the x-ray spectrum. The samples with nanoclay, on the other hand are observed to have a diffraction peak corresponding to 17.6 Å gallery spacing, regardless of the nanoclay content. This 48% increase in gallery spacing of nanoclay is a clear indication of intercalation. The epoxy molecules must have penetrated between the clay sheets and result in the expansion in gallery spacing.

The mechanics of nanoclay intercalation with polymers to form nanocomposites is rather complex. Intercalation is not only controlled by the diffusion rate of the epoxy and curing agent molecules, but also by the balance of intra- and extra-gallery polymerization [38]. If the polymerization initiates at the extra-gallery regions before epoxy molecules diffuse completely into the intra-gallery regions, the expansion of the gallery space will not be completely achieved and an intercalated structure will form. An affirming observation stressing the initiation of polymerization was made by Raghavan et al. [43]. The authors report that mixing organically modified nanoclay in DGEBA epoxy resin yielded intercalation as indicated by the shift in XRD spectra. However, allowing the nanoclay to swell in hot epoxy resin for several hours resulted in complete exfoliation. The gel time of the composite laminates currently studied was measured as 25 min. This duration may not be adequate for the epoxy molecules to completely diffuse into the intra-gallery regions of the nanoclay structure.

Mechanical Properties

The average values of flexural stiffness and interlaminar shear strength are given in Fig. 6. The interlaminar shear strength of the composite samples decreased monotonically from 18.6 MPa to 14.9 MPa when the nanoclay content is increased to 4 wt%. Corroborating our findings, the interlaminar shear strength of samples with identical glass fiber reinforcement was measured by Olivero et al. [44] as 17 MPa. On the other hand, flexural stiffness displayed considerable increase over the range of nanoclay loading. The flexural stiffness for the composite sample without nanoclay is measured as 11.2 GPa. The flexural stiffness increased to 12.9 GPa at 1 wt%, 13 GPa at 2 wt% and 14.2 GPa at 4 wt% nanoclay loading. This 26% increase in flexural stiffness is beyond the uncertainty of the experiments as dictated by the 95% confidence interval error bars.

Mechanical property improvements due to nanoclay are reported more frequently for weak polymers such as

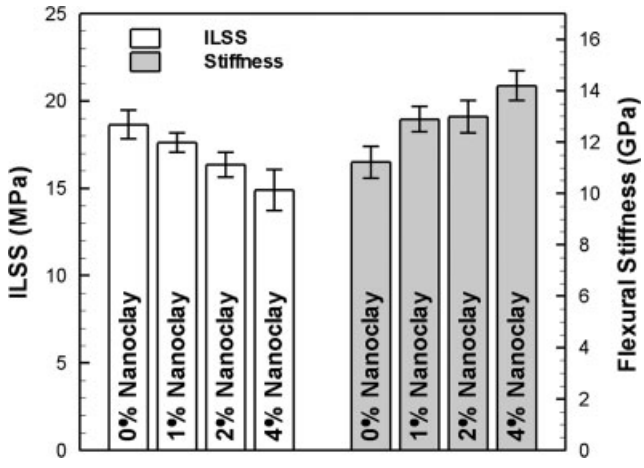

FIG. 6. Interlaminar shear strength and flexural stiffness of composite samples with various nanoclay contents.

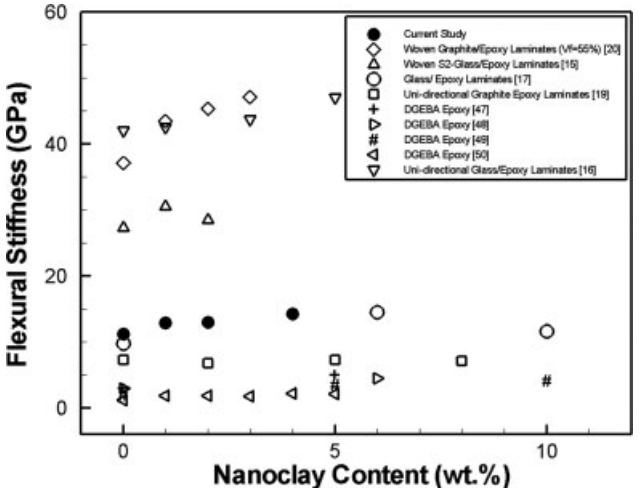

FIG. 7. Flexural stiffness values for nanoclay/epoxy composites reported in literature.

thermoplastics and rubbery epoxies. For instance, the tensile modulus of 3 MPa for the epoxy matrix without nanoclay increased to 35 MPa at 23.2 wt% loading as reported by Lan and Pinnavaia [21]. Similarly, the tensile modulus for the neat epoxy in the case of Boukerrou et al. [22] was reported to change from 0.56 MPa to 0.76 MPa at 5 wt% nanoclay loading. Considering that the elastic moduli values of nanoclay platelet is reported to be ranging between 20 and 400 GPa [45], such improvements are not surprising [46]. However, even after such improvements, the performance of these polymers is superseded by composites comprising conventional fiber reinforcements.

The flexural stiffnesses of various composites and epoxy polymers containing nanoclay [15–18, 20, 47-50] are given in Fig. 7. The lower end of the flexural stiffness spectrum is populated by studies dealing with epoxy polymers without fibers. Composites containing glass or graphite fibers are located above the polymers. On the high end of the flexural stiffness spectrum are the composites containing ordered (woven or unidirectional) glass and graphite fibers. Clearly, mechanical properties that are superior than nanoclay reinforced rubbery epoxies can readily be achieved with the use of conventional fiber reinforcements. Considering that the carbon fibers have modulus values ranging between 200 and 700 GPa and E-glass fibers have a modulus of 76 GPa [51], enhancement of the stiffness of fiber reinforced composites due to nanoclay is most often moderate. However, using small amounts of nanoclay in epoxy based composites to capture this 20%–40% stiffness improvement is likely to be more cost-effective compared with increasing the fiber volume fraction of the composite. Adding nanoclay will also have other benefits such as reduced moisture absorption, improved flame retardancy, and thermal stability.

To better compare the effects of nanoclay on the performance of the composites used in the current study, relative percentage improvement in flexural stiffness of epoxy matrix composites, excluding the neat polymers, is shown in Fig. 8. It is observed from Fig. 8 that the percentage improvement in flexural stiffness of our samples is higher than majority of the previous studies. For example, flexural stiffness of unidirectional glass/epoxy laminates improved by 12% with the addition of nanoclay as reported by Lin et al. [16], whereas the nanocomposite samples fabricated in this study achieved almost 30% improvement at 4% nanoclay loading. The improvement observed in the current study is most likely due to (i) increased nanoclay gallery spacing as shown in Fig. 5 and (ii) homogoeneous dispersion of nanoclay by the aqueous solution; hence, leading to uniform distribution of nanoclay throughout the waterborne epoxy matrix. Achieving stiffness improvement up to 30% also suggests the possibility of having uniformly dispersed, submicron nanoclay clusters, as mechanical performance is known to be highly dependent on the particle size [52–54].

Glass Transition Temperature

There are three indications of glass transition temperature when measured by DMA: (i) a sharp drop in storage modulus with increasing temperature, (ii) the peaks displayed by loss tangent and (iii) loss modulus. The change in storage modulus along with the loss tangent during glass transition is shown in Fig. 9. It is interesting to observe that after glass transition, the samples containing nanoclay are observed to maintain their stiffness more efficiently. For instance, the ratio of storage modulus of composite sample containing 4 wt% nanoclay to the one without at 60°C is 1.03. After glass transition, the same ratio increases to 3.39 at 125°C. Therefore, for applications requiring elevated temperatures, addition of nanoclay to the composites presents a clear advantage.

The glass transition temperature of the polymers and composites indicate the temperature at which a relaxation

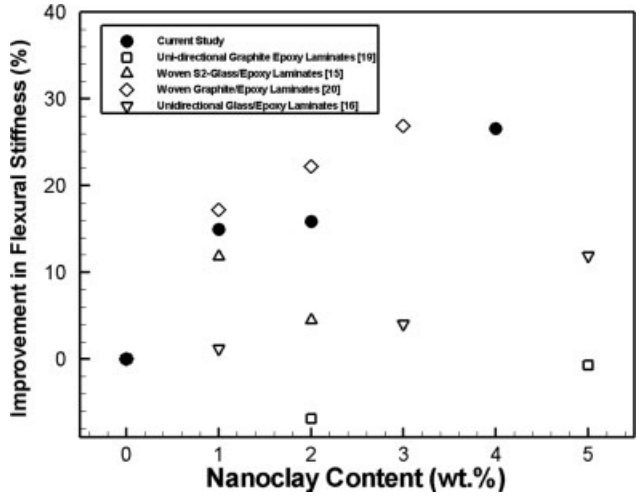

FIG. 8. Improvement in flexural stiffness of various composites with nanoclay content.

 DOI 10.1002/pc

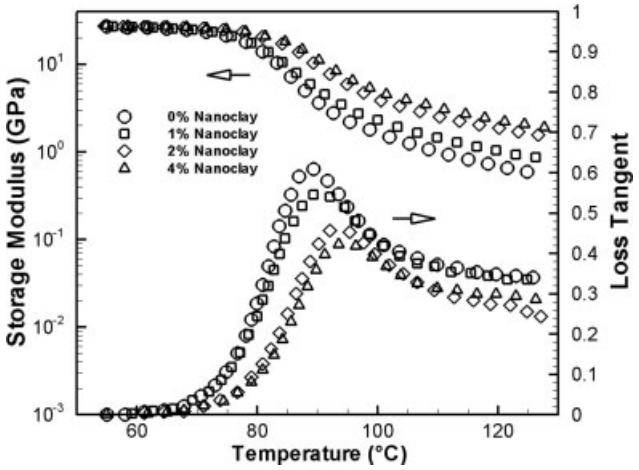

FIG. 9. Change in storage modulus and loss tangent during glass transition.

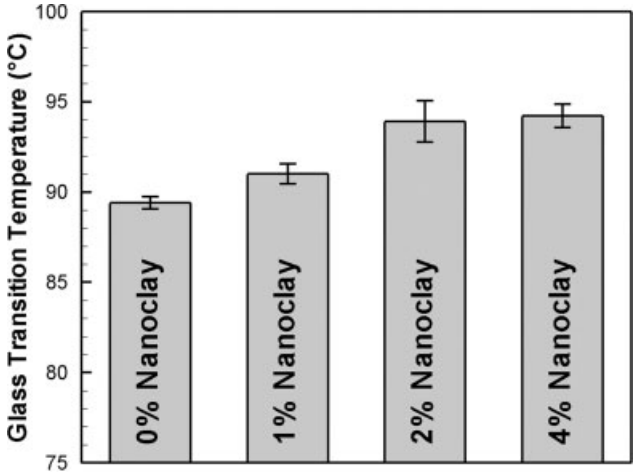

FIG. 10. Glass transition temperature values obtained from by the peak loss tangent method.

at molecular level takes place. Therefore, as indicated by Tien and Wei [55], the glass transition temperature increases if the molecular motion is hindered by the nanoclay platelets, which also is an indication of strong intercalation. In the current study, the temperature at which the loss tangent displays a peak is reported as the glass transition temperature. The glass transition temperature values along with 95% confidence intervals are given in

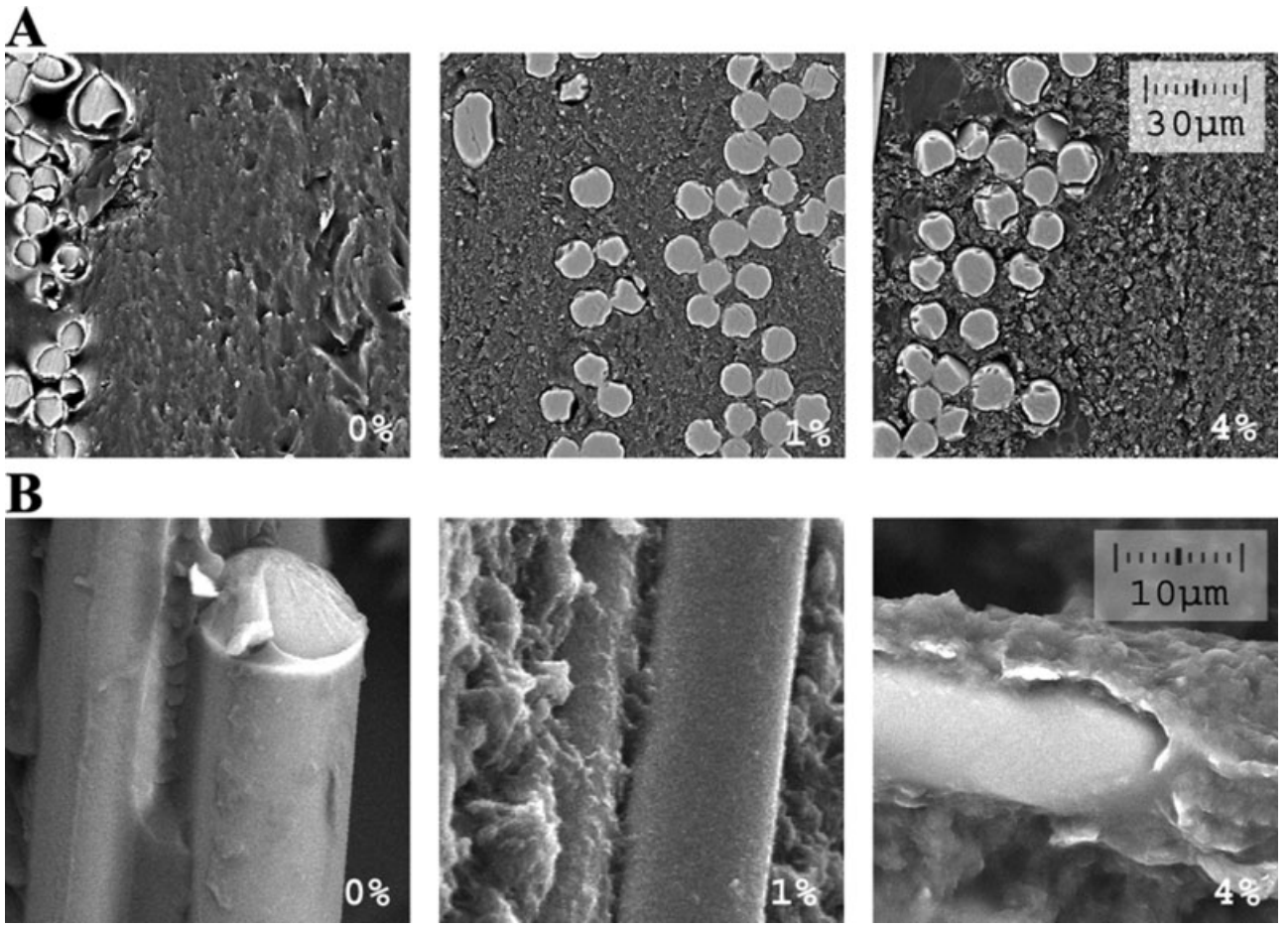

FIG. 11. Scanning electron micrographs of composite samples with 0, 1, and 4 wt% nanoclay. (A) Images taken at ×250 from the polished surfaces (Top). (B) Fracture surface images taken at ×1000 (Bottom).

Fig. 10. The glass transition temperature increased monotonically with increasing nanoclay content. At the maximum nanoclay loading of 4 wt%, the glass transition temperature displayed an increase of 5% from 89.4°C to 94.2°C.

It is reported that at cure temperatures higher than thermal dissociation temperature of alkyl ammonium ions used in the cation exchange of layered silicates, primary amines are generated [56]. The generation of primary amines gives rise to epoxy self-polymerization and thus yields excess curing agent and significant reductions in glass transition temperature [29]. The use of natural nanoclay in the current study most likely eliminated this problem, which may have been observed in the organoclay based nanocomposites.

Microstructure

The scanning electron micrographs of the polished composite samples and the fracture surfaces are shown in Fig. 11. It is often not possible to see individual nanoclay platelets embedded in a polymer matrix using scanning electron microscopy. However, the surface properties observed in polished nanocomposite samples is an indication of the homogeneity of the nanoclay dispersion. The scanning electron micrographs of the polished surfaces of the samples with 0, 1, and 4 wt% nanoclay are shown in Fig. 11A. Compared with the sample without nanoclay, samples containing 1 and 4 wt% nanoclay display a granular surface topology with geometric features at smaller length scales. In addition, the surface roughness is observed to increase with increasing nanoclay content. Microstructural differences similar to the ones observed herein have been reported elsewhere for vacuum assisted resin transfer molded glass/epoxy composites [16] and pressed carbon/epoxy composites [57] containing nanoclay. These differences in surface topologies are most likely due to the presence of nanoclay clusters. The uniformity of the surface characteristics of the samples as observed in low magnification SEM images shown in Fig. 11B indicates that nanoclay dispersed uniformly within the epoxy matrix.

Similar to the polished surfaces, scanning electron micrographs of the fracture surfaces are notably different. A fiber bundle from the fracture surface of the composite sample without nanoclay is shown in Fig. 11B. Matrix residues that are observed on the fiber surfaces and between fibers are unequivocal signs of good fiber-matrix adhesion. Figure 11B also shows the fracture surfaces of the composite samples with 1 and 4 wt% nanoclay. It is interesting to note that the fiber matrix interface contains more matrix material compared to the sample without nanoclay. Especially the buildup of matrix material around the fibers is notable. Existence of matrix material around the fibers after fracture indicates that effective fiber-matrix adhesion is maintained after the addition of nanoclay.

CONCLUSION

A new method to fabricate E-glass/nanoclay/waterborne epoxy prepregs by using an aqueous solution is presented. The prepregs are prepared by wetting randomly oriented, chopped E-glass fiber preforms by an aqueous dispersion of EpiRez 3522-W-60 waterborne epoxy resin, dicyandiamide and 2-methylimidazole. Various amounts of natural nanoclay (Cloisite® Na^+) is added to yield a final matrix nanoclay content of 0, 1, 2, and 4 wt%. Using the fabricated prepregs, disk-shaped 14-ply laminates are cured by a rheometer.

X-ray diffraction studies of the composite samples revealed a 48% increase in the gallery spacing of the nanoclay, thus indicating effective intercalation of nanoclay platelets by the epoxy matrix. Despite a 13.5% decrease in interlaminar shear strength, the flexural stiffness was observed to increase by more than 26% over the range of nanoclay loading. Glass transition temperature is measured to increase by more than 5% from 89.4°C at 0 wt% to 94.2°C at 4 wt%. Scanning micrographs also revealed improved adhesion of fibers to the matrix material with increasing nanoclay content.

REFERENCES

1. K.K. Maniar, *Polym. Plast. Technol. Eng.*, **43**, 427 (2004).
2. P.C. LeBaron, Z. Wang, and T.J. Pinnavaia, *Appl. Clay Sci.*, **15**, 11 (1999).
3. S.J. Ahmadi, Y.D. Huang, and W. Li, *J. Mater. Sci.*, **39**, 1919 (2004).
4. T.J. Pinnavaia, *Polymer-clay Nanocomposites*, Wiley: New York (2000).
5. A. Usuki, M. Kawasumi, Y. Kojima, A. Okada, T. Kurauchi, and O. Kamigaito, *J. Mater. Res.*, **8**, 1174 (1993).
6. A. Usuki, Y. Kojima, M. Kawasumi, A. Okada, Y. Fukushima, T. Kurauchi, and O. Kamigaito, *J. Mater. Res.*, **8**, 1179 (1993).
7. Y. Kojima, A. Usuki, M. Kawasumi, A. Okada, Y. Fukushima, T. Kurauchi, and O. Kamigaito, *J. Mater. Res.*, **8**, 1185 (1993).
8. J.W. Cho and D.R. Paul, *Polymer*, **42**, 1083 (2001).
9. L. Chen, S.C. Wong, and S. Pisharath, *J. Appl. Polym. Sci.*, **88**, 3298 (2003).
10. B.N. Jang and C.A. Wilkie, *Polymer*, **46**, 2933 (2005).
11. T. Kashiwagi, R.H. Harris, X. Zhang, R.M. Briber, B.H. Cipriano, S.R. Raghavan, W.H. Awad, and J.R. Shields, *Polymer*, **45**, 881 (2004).
12. K. Yano, A. Usuki, A. Okada, T. Kurauchi, and O. Kamigaito, *J. Polym. Sci.Part A: Polym. Chem.*, **31**, 2493 (1993).
13. E. Petrovicova, R. Knight, L.S. Schadler, and T.E. Twardowski, *J. Appl. Polym. Sci.*, **78**, 2272 (2000).
14. P. Maiti, P.H. Nam, M. Okamoto, N. Hasegawa, and A. Usuki, *Macromolecules*, **35**, 2042 (2002).
15. A. Haque, M. Shamsuzzoha, F. Hussain, and D. Dean, *J. Compos. Mater.*, **37**, 1821 (2003).

 DOI 10.1002/pc

16. L.Y. Lin, J.H. Lee, C.E. Hong, G.H. Yoo, and S.G. Advani, *Compos. Sci. Technol.*, **66**, 2116 (2006).
17. L.H. Nguyen, D.T. Nguyen, T.H. La, K.X. Phan, T.T.T. Nguyen, and H.N. Nguyen, *J. Appl. Polym. Sci.*, **103**, 3238 (2007).
18. J.F. Timmerman, B.S. Hayes, and J.C. Seferis, *Compos. Sci. Technol.*, **62**, 1249 (2002).
19. J.F Timmerman, B.S. Hayes, and J.C. Seferis, "Cryogenic Microcracking of Nanoclay Reinforced Polymeric Composite Materials," in *47th International SAMPE Symposium*, Long Beach, CA, 1119 (2002).
20. F.H. Chowdhury, M.V. Hosur, and S. Jeelani, *J. Mater. Sci.*, **42**, 2690 (2007).
21. T. Lan and T.J. Pinnavaia, *Chem. Mater.*, **6**, 2216 (1994).
22. A. Boukerrou, J. Duchet, S. Fellahi, M. Kaci, and H. Sautereau, *J. Appl. Polym. Sci.*, **103**, 3547 (2007).
23. J.L. Abot, A. Yasmin, and I.M. Daniel, *Mater. Res. Soc. Symp. Proc.*, **740**, I6.5.1 (2003).
24. K. Wang, J. Wu, L. Chen, C. He, and M. Toh, "Mechanical Properties and Fracture Behavior of Epoxy Nanocomposites with Highly Exfoliated Pristine Clay," in *Annual Technical Conference, Society of Plastics Engineers*, Chicago, IL, 1820 (2004).
25. H. van Olphen, *An Introduction to Clay Colloid Chemistry*, Wiley: New York (1977).
26. EpiRez 3522-W-60, Materials Data Sheet, Columbus, OH, Hexion Chemicals Inc.
27. Y.K. Hamidi, L. Aktas, and M.C. Altan, *J. Thermoplas. Compos.*, **21**, 141 (2005).
28. T. Lan, D. Kaviratna, and T.J. Pinnavaia, *J. Phys. Chem. Solids*, **57**, 1005 (1996).
29. J. Park and S.C. Jana, *Macromolecules*, **36**, 8391 (2003).
30. L. Aktas, S. Dharmavaram, Y.K. Hamidi, and M.C. Altan, "Characterization of Nanoclay Dispersion in Epoxy Matrix by Combined Image Analysis and Wavelength Dispersive Spectrometry," in *22nd Annual Meeting of Polymer Processing Society*. Paper no.:SP4.28. Yamagata, Japan (2007).
31. M. Hargis, B.P. Grady, L. Aktas, K.R. Bomireddy, S. Howsman, M.C. Altan, T. Rose, and H. Rose, *J. Compos. Mater.*, **40**, 873 (2006).
32. X. Ramis, A. Cadenato, J.M. Morancho, and J.M. Salla, *Polymer*, **44**, 2067 (2003).
33. A.Y. Malkin, I.Y. Gorbunova, and M.L. Kerber, *Polym. Eng. Sci.*, **45**, 95 (2005).
34. G. Kortaberria, L. Solar, A. Jimeno, P. Arruti, C. Gomez, and I. Mondragon, *J. Appl. Polym. Sci.*, **102**, 5927 (2006).
35. F.M. Uhl, S.P. Davuluri, S.C. Wong, and D.C. Webster, *Chem. Mater.*, **16**, 1135 (2004).
36. K.S. Seo and D.S. Kim, *Polym. Eng. Sci.*, **46**, 1318 (2006).
37. F. Roman, S. Montserrat, and J.M. Hutchinson, *J. Therm. Anal. Calorimetry*, **87**, 113 (2007).
38. X. Kornmann, H. Lindberg, and L.A. Berglund, *Polymer*, **42**, 4493 (200).
39. T.D. Ngo, M.T. Ton-That, S.V. Hoa, and K.C. Cole, *Polym. Eng. Sci.*, **47**, 649 (2007).
40. W.H. Bragg and W.L. Bragg, *Proc. R. Soc. London Ser. A*, **88**, 428 (1913).
41. X. Kornmann, H. Lindberg, and L.A. Berglund, *Polymer*, **42**, 1303 (2001).
42. Cloisite® Na+, Materials Data Sheet, Gonzales, TX, Southern Clay Products Inc.
43. D. Raghavan, E. Feresenbet, D. Yebassa, A. Emelkalam, and G. Holmes, *Mater. Res. Soc. Symp. Proc.*, **703**, V9.26.1 (2002).
44. K.A. Olivero, Y.K. Hamidi, L. Aktas, and M.C. Altan, *J. Compos. Mater.*, **38**, 937 (2004).
45. B.Q. Chen and J.R.G. Evans, *Scripta Materialia*, **54**, 1581 (2006).
46. T.D. Ngo, M.T. Ton-That, S.V. Hoa, and K.C. Cole, "Rubbery and Glassy Epoxy-Clay Nanocomposites," in *Proceedings of the Sixth Joint Canada-Japan Workshop on Composites. Design, Manufacturing and Applications of Composites*, Toronto, ON, Canada, 112 (2006).
47. D. Ratna, O. Becker, R. Krishnamurthy, G.P. Simon, and R.J. Varley, *Polymer*, **44**, 7449 (2003).
48. C.S. Triantafillidis, P.C. LeBaron, and T.J. Pinnavaia, *Chem. Mater.*, **14**, 4088 (2002).
49. J. Massam, T.J. Pinnavaia, *Mater. Res. Soc. Symp. Proc.*, **520**, 223 (1998).
50. S. McIntyre, I. Kaltzakorta, J.J. Liggat, R.A. Pethrick, and I. Rhoney, *Ind. Eng. Chem. Res.*, **44**, 8573 (2005).
51. R.F. Gibson, *Principles of Composite Material Mechanics*, McGraw-Hill Inc: New York (1994).
52. R.J. Cardoso, A. Shukla, and A. Bose, *J. Mater. Sci.*, **37**, 603 (2002).
53. R.P. Singh, M. Zhang, and D. Chan, *J. Mater. Sci.*, **37**, 781 (2002).
54. C.R. Siviour, M.J. Gifford, S.M. Walley, W.G. Proud, and J.E. Field, *J. Mater. Sci.*, **39**, 1255 (2004).
55. Y.I. Tien and K.H. Wei, *J. Appl. Polym. Sci.*, **86**, 1741 (2002).
56. J. Park and S.C. Jana, *Polymer*, **45**, 7673 (2004).
57. O. Becker, R.J. Varley, and G.P. Simon, *J. Mater. Sci. Lett.*, **22**, 1411 (2003).